ROYAL SOCIETY OF CHEMISTRY

www.rsc.org/advances

A series of rare-earth substituted dimeric complexes of Keggin-type silicotungstates were synthesized and characterized using various analytical techniques like SCXD, Photoluminescence, ^{1}H and ^{13}C NMR spectroscopy.
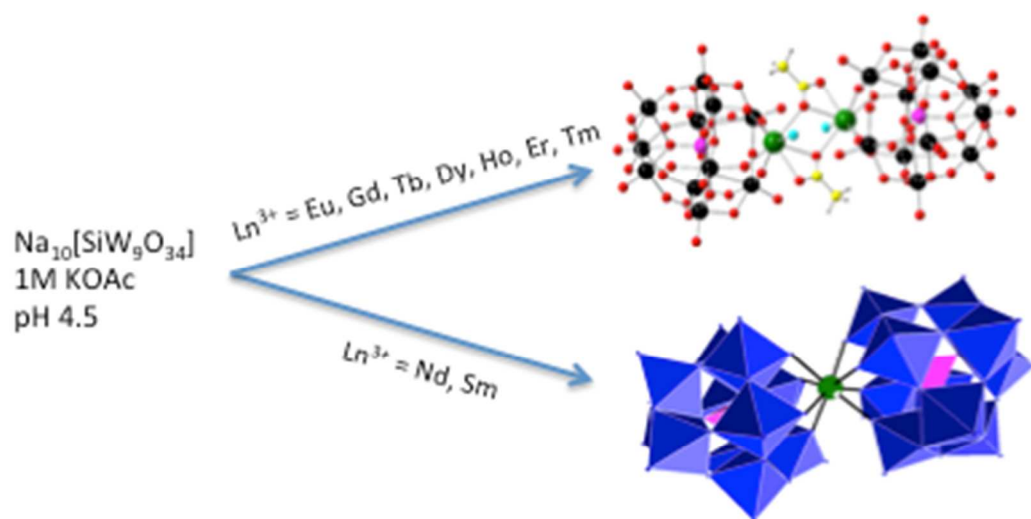
Dimeric complexes of rare-earth substituted Keggin-type silicotungstates: Syntheses, crystal structure and solid state properties

Mukesh Kumar Saini,[a] **Rakesh Gupta,**[a] **Swati Parbhakar,**[a] **Anil Kumar Mishra,**[b] **Rashi Mathur,**[b] **and Firasat Hussain***[a]

A series of rare-earth substituted dimeric complexes of Keggin-type silicotungstates: $[\{Ln(\alpha\text{-}SiW_{11}O_{39})(H_2O)\}_2(\mu\text{-}CH_3COO)_2]^{12-}$ [Ln = Eu^{III} (**Eu-1**), Gd^{III} (**Gd-2**), Tb^{III} (**Tb-3**), Dy^{III} (**Dy-4**), Ho^{III} (**Ho-5**), Er^{III} (**Er-6**) and Tm^{III} (**Tm-7**)] and $[Ln(\alpha\text{-}SiW_{11}O_{39})_2]^{13-}$ [Ln = Pr^{III} (**Pr-8**), Nd^{III} (**Nd-9**), Sm^{III} (**Sm-10**)] were synthesized by a single step reaction of $Na_{10}[\alpha\text{-}SiW_9O_{34}]\cdot16H_2O$ with $Ln(NO_3)_3\cdot nH_2O$ in potassium acetate buffer at pH 4.5. All these compounds were structurally characterized by single-crystal X-ray diffraction, and other analytical techniques including FT-IR, ICP-AES, UV/vis, photoluminescence spectroscopy, thermogravimetric analysis, ^{13}C and ^{1}H NMR spectroscopy and vibrating sample magnetometry (VSM). The single-crystal X-ray diffraction and FT-IR studies suggest that the compounds (**Eu-1a – Tm-7a**), and (**Pr-8a – Sm-10a**) are isostructural. The photoluminescence properties of **Eu-1a**, **Tb-3a**, **Dy-4a** and **Sm-10a** were studied at room temperature. VSM studies of **Gd-2a**, **Tb-3a**, **Dy-4a**, **Ho-5a**, **Er-6a** and **Tm-7a** were studied at room temperature, shows paramagnetic behaviour.

Introduction

Polyoxometalates (POMs) are oxo-clusters generally composed of early transition metals in their highest oxidation states. POMs show a wide structural diversity which make its very useful in the area of catalysis, medicine, molecular magnets, imaging techniques, biotechnology and nanomaterials design, and this attracts the worldwide research attention in the area of POMs.[1-10] Due to its simple synthetic strategy so many POM aggregates of transition metals and rare-earth metals had been synthesized. In this series polyoxotungstoaresenate (III) $[Ce_{16}As_{12}(H_2O)_{36}W_{148}O_{524}]^{76-}$ discovered by Pope at al. in 1997, still remains the largest discrete polyoxotungstate known to date[11]. Later on another Cerium-containing POM $[Ce_{20}Ge_{10}W_{100}O_{376}(OH)_4(H_2O)_{30}]^{56-}$ was reported by Kortz et al.

as the second largest representative of POMs[12]. Recently, one of us extended the linking affinity of mid and late lanthanides and reported on $[Ln_{16}As_{16}W_{164}O_{576}(OH)_8(H_2O)_{42}]^{80-}$ (Ln = Eu, Gd, Tb, Dy and Ho), which is the largest polyoxotungstate known to date in terms of tungsten centres.[13d]

Lanthanoid cations are very reactive to the Keggin-type POM ligands due to their high co-ordination numbers and large oxophilicity, leading to the formation of variety of lanthanoid substituted POMs[13]. Peacock and Weakley studied the interactions between four identical isomers of the $[SiW_{11}O_{39}]^{8-}$ polyanion and lanthanoid cations and they found that the $[\alpha-SiW_{11}O_{39}]^{8-}$ forms both 1:1 and 1:2 compounds with rare-earth metals[14]. Later, Pope et al. studied the structural characterization of the polymeric silicoanions 1D - $[Ln(\alpha-SiW_{11}O_{39})(H_2O)_3]^{5-}$ (Ln = La^{III}, Ce^{III}) in the solid state and concluded that both the Cerium and Lanthanum compounds were closely related but with some differences, like Cerium POM having an inversion centre and Lanthanum POM exists without inversion centre, in addition they showed decrease in lanthanoid source leads to the formation of $[Ln(SiW_{11}O_{39})_2]^{13-}$ (Ln = La and Ce) dimer as side product[15]. Mialane et al. reported the solid-state structure of the Ln/$[\alpha-SiW_{11}O_{39}]^{8-}$ (Ln = Yb^{III}, Nd^{III}, Eu^{III} and Gd^{III}) and investigated that these compounds strongly depended on the kind of lanthanide cation used[16]. Later, Mialane et al. also reported the structural characterization of compounds $K_{12}[\{Ln(\alpha-SiW_{11}O_{39})(H_2O)\}_2(\mu-CH_3COO)_2]\cdot38H_2O$ (Ln = Gd^{III}, Yb^{III}) with rare-earth acetate bridged between two monolacunary silicoanions, but no crystal structure was reported for Gd^{III} complex[17]. Niu's group also reported on 1D chainlike $K_3[(Pr(H_2O)_4SiW_{11}O_{39})(NaPr_2(H_2O)_{12}(Pr(H_2O)_4SiW_{11}O_{39})]\cdot13\cdot5H_2O$ silicotungstate with sodium ion as the bridging centre, they also reported the three 1D and 2D organic-inorganic hybrid monovacant Keggin-type silicotungstate and germanotungstate with the linkage of rare-earth metal with organic cations[18,19]. In 2006, Lin Xu and co-workers reported $K[Ln_2(\alpha-SiW_{11}O_{39})(H_2O)_{11}]$ (Ln = La, Ce) one dimensional chain based POMs using the Ni-substituted polyoxometalate as the starting material[20]. Likewise in 2007, Kortz et al. reported a family of monolanthanide substituted Keggin-type silicotungstates $[Ln(\beta_2-SiW_{11}O_{39})_2]^{13-}$ (Ln = La^{3+}, Ce^{3+}, Sm^{3+}, Eu^{3+}, Gd^{3+}, Tb^{3+}, Yb^{3+} and Lu^{3+}) in which lanthanide cation located in between two monolacunary silicoanions in sandwich type[21]. In 2010, Dongying and co-workers synthesized a family of inorganic-organic hybrid

nanoclusters $[Cu(en)_2H_2O]_3[(\alpha-SiW_{11}O_{39})Ln(H_2O)(\eta^2,\mu-1,1)-CH_3COO]\cdot nH_2O$ (Ln = Nd, Sm) (en-1,2-ethylenediamine), in a one dimensional ladder like manner constructed from $[(\alpha-SiW_{11}O_{39})Ln(H_2O)(\eta^2,\mu-1,1)-CH_3COO]^{6-}$ polyanion and $[Cu(en)_2H_2O]^{2+}$ cations[22]. Recently in 2012, Haiyan An and his research group first reported the 3D inorganic framework based on 2:2 type lanthanide substituted Keggin-type silicotungstates $KLn[(H_2O)_6Ln]_2[(H_2O)_4LnSiW_{11}O_{39}]_2\cdot nH_2O$ (Ln = La, Ce)[23]. Very recently, Patzke et al. reported a new complex $[Eu(\alpha-SiW_{11}O_{39})_2]^{13-}$ containing monolacunary Keggin-type anion[24]. Niu's group and one of us reported a series of similar complexes as mentioned here, with phosphotungstates[25] and germanotungstates[13f] respectively.

Herein, we report on new examples of the seven acetate bridged lanthanoid substituted $[\{Ln(\alpha-SiW_{11}O_{39})(H_2O)\}_2(\mu-CH_3COO)_2]^{12-}$ [Ln = Eu^{III} (**Eu-1**), Gd^{III} (**Gd-2**), Tb^{III} (**Tb-3**), Dy^{III} (**Dy-4**), Ho^{III} (**Ho-5**), Er^{III} (**Er-6**) and Tm^{III} (**Tm-7**)], and three $[Ln(\alpha-SiW_{11}O_{39})_2]^{13-}$ (Ln = Pr^{III} (**Pr-8**), Nd^{III} (**Nd-9**), Sm^{III} (**Sm-10**) dimeric silicotungstates.

Experimental section

General: The trilacunary $Na_{10}[A-\alpha-SiW_9O_{34}]\cdot16H_2O$ was prepared according to the published literature[26] procedure and its purity was confirmed by FT-IR spectrum. All other chemicals were commercially purchased and were used without further purification. The Fourier transform (FT-IR) spectra were recorded with Perkin-Elmer BX spectrum on KBr pellets. Thermogravimetric analysis (TGA) were performed using a TG/DTA instrument DTG-60 Shimadzu between temperature range of 25-700 °C in a nitrogen atmosphere with a heating rate of 5 °C/min. Solid UV/vis spectra were recorded on a Thermo Scientific Evolution 300 spectrometer. Elemental analysis was performed using an ICP-AES instrument, ARCOS from M/s Spectro Germany. All the ^{13}C and ^1H -NMR spectra were recorded with a Jeol ECX 400P spectrometer at 400 MHz magnetic field in 9.38T field strength. Photoluminescence measurements were performed on a Fluorolog Horiba Jobinyvon spectrometer. Single-crystal X-ray diffraction (SCXRD) data were recorded on a Xcalibur Oxford Diffractometer, using 50 kV and 40 mA (Mo Kα1 radiation). The magnetic measurements were performed using a Microsense ADE-EV9 vibrating sample magnetometer.

Na$_4$K$_8$[{Eu(α-SiW$_{11}$O$_{39}$)(H$_2$O)}$_2$(μ-CH$_3$COO)$_2$]·28H$_2$O (Eu1a):

0.1284 g (0.3 mmol) of Eu(NO$_3$)$_3$·6H$_2$O was dissolved in 25 ml of 1M potassium acetate buffer at pH 4.5. Then the 0.2546 g (0.1 mmol) of Na$_{10}$[A-α-SiW$_9$O$_{34}$]·16H$_2$O, was slowly added to the above solution with continuous stirring, and was heated at 50 ºC for 30 min. The solution was filtered after cooling down to the room temperature and was set aside for crystallization under the ambient conditions. After 5-6 weeks, diamond-shaped single crystals were collected with a yield of 0.1520 g, 60% (based on Na$_{10}$[α-SiW$_9$O$_{34}$]·16H$_2$O). FT-IR: 1624(s), 1528(m), 1437(m), 1398(m), 1003(m), 953(s), 905(s), 886(s), 807(w), 755(sh), 695(m), 675(m), 540(m), 523(m), 482(w) (cm^{-1}). Elemental analysis (%); calcd. (found): Na 1.4 (1.6), K 4.7 (4.5), W 60.3 (58.7).

Na$_4$K$_8$[{Gd(α-SiW$_{11}$O$_{39}$)(H$_2$O)}$_2$(μ-CH$_3$COO)$_2$]·22H$_2$O (Gd-2a):

The above synthetic procedure was followed by using 0.1354 g (0.3 mmol) of Gd(NO$_3$)$_3$·6H$_2$O instead of Eu(NO$_3$)$_3$·6H$_2$O. Yield: 0.1468 g, 58% (based on Na$_{10}$[α-SiW$_9$O$_{34}$]·16H$_2$O). FT-IR: 1624(s), 1527(m), 1438(m), 1398(m), 1005(m), 953(s), 907(s), 885(s), 808(w), 759(sh), 697(m), 677(m), 539(m), 519(m), 483(w) (cm^{-1}). Elemental analysis (%); calcd. (found): Na 1.4 (1.9), K 4.7 (4.3), W 61.1 (59.2).

Na$_4$K$_8$[{Tb(α-SiW$_{11}$O$_{39}$)(H$_2$O)}$_2$(μ-CH$_3$COO)$_2$]·22H$_2$O (Tb-3a):

The above synthetic procedure was followed by using 0.1305 g (0.3 mmol) of Tb(NO$_3$)$_3$·5H$_2$O instead of Eu(NO$_3$)$_3$·6H$_2$O. Yield: 0.1483 g, 58% (based on Na$_{10}$[α-SiW$_9$O$_{34}$]·16H$_2$O). FT-IR: 1624(s), 1533(m), 1450(m), 1398(m), 1005(m), 953(s), 906(s), 886(s), 811(w), 757(sh), 699(m), 678(m), 540(m), 525(m), 482(w) (cm^{-1}). Elemental analysis (%); calcd. (found): Na 1.4 (1.7), K 4.7 (4.3), W 61.1 (59.0).

Na$_4$K$_8$[{Dy(α-SiW$_{11}$O$_{39}$)(H$_2$O)}$_2$(μ-CH$_3$COO)$_2$]·30H$_2$O (Dy-4a):

The above synthetic procedure was followed by using 0.1315 g (0.3 mmol) of Dy(NO$_3$)$_3$·H$_2$O instead of Eu(NO$_3$)$_3$·6H$_2$O. Yield: 0.1512 g, 59% (based on Na$_{10}$[α-

SiW$_9$O$_{34}$]·16H$_2$O). FT-IR: 1624(s), 1533(m), 1438(m), 1398(m), 1006(m), 952(s), 908(s), 888(s), 810(w), 757(sh), 697(m), 677(m), 540(m), 523(m), 482(w) (cm^{-1}). Elemental analysis (%); calcd. (found): Na 1.36 (1.7), K 4.6 (4.4),W 59.7 (57.2).

Na$_4$K$_8$[{Ho(α-SiW$_{11}$O$_{39}$)(H$_2$O)}$_2$(μ-CH$_3$COO)$_2$]·26H$_2$O (Ho-5a):

The above synthetic procedure was followed by using 0.1323 g (0.3 mmol) of Ho(NO$_3$)$_3$·5H$_2$O instead of Eu(NO$_3$)$_3$·6H$_2$O. Yield: 0.1397 g, 55% (based on Na$_{10}$[α-SiW$_9$O$_{34}$]·16H$_2$O). FT-IR: 1622(s), 1534(m), 1450(m), 1398(m), 1007(m), 952(s), 908(s), 890(s), 811(w), 759(sh), 698(m), 679(m), 540(m), 524(m), 482(w) (cm^{-1}). Elemental analysis (%); calcd. (found): Na 1.37 (1.8), K 4.7 (4.1),W 60.3 (57.9).

Na$_4$K$_8$[{Er(α-SiW$_{11}$O$_{39}$)(H$_2$O)}$_2$(μ-CH$_3$COO)$_2$]·26H$_2$O (Er-6a):

The above synthetic procedure was followed by using 0.1330 g (0.3 mmol) of Er(NO$_3$)$_3$·5H$_2$O instead of Eu(NO$_3$)$_3$·6H$_2$O. Yield: 0.1506 g, 59% (based on Na$_{10}$[α-SiW$_9$O$_{34}$]·16H$_2$O). FT-IR: 1623(s), 1534(m), 1449(m), 1399(m), 1008(m), 952(s), 909(s), 891(s), 812(w), 759(sh), 699(m), 679(m), 540(m), 524(m), 482(w) (cm^{-1}). Elemental analysis (%); calcd. (found): Na 1.37 (1.7), K 4.7 (4.3), W 60.3 (58.3).

Na$_4$K$_8$[{Tm(α-SiW$_{11}$O$_{39}$)(H$_2$O)}$_2$(μ-CH$_3$COO)$_2$]·26H$_2$O (Tm-7a):

The above synthetic procedure was followed by using 0.1335 g (0.3 mmol) of Tm(NO$_3$)$_3$·5H$_2$O instead of Eu(NO$_3$)$_3$·6H$_2$O. Yield: 0.1369 g, 54% (based on Na$_{10}$[α-SiW$_9$O$_{34}$]·16H$_2$O). FT-IR: 1623(s), 1537(m), 1453(m), 1398(m), 1008(m), 952(s), 911(s), 891(s), 814(w), 759(sh), 699(m), 680(m), 541(m), 524(m), 482(w) (cm^{-1}). Elemental analysis (%); calcd. (found): Na 1.37 (1.8), K 4.7 (4.3),W 60.2 (58.1).

K$_6$Na$_7$[Pr(SiW$_{11}$O$_{39}$)$_2$]·20H$_2$O (Pr-8a): 0.1305 g (0.3 mmol) of Pr(NO$_3$)$_3$·6H$_2$O was dissolved in 25 ml of 1M potassium acetate buffer at pH 4.5. Later, 0.2546 g (0.1 mmol) of Na$_{10}$[A-α-SiW$_9$O$_{34}$]·16H$_2$O, was slowly added in the above solution with continuous stirring, and heated at 50 C for 30 min. The solution was filtered after cooling down to the room temperature and was set aside for crystallization under the ambient conditions. After 4-5 weeks parallelepiped-shaped single crystals were obtained, Yield: 0.1397 g,

55% (based on $Na_{10}[\alpha\text{-}SiW_9O_{34}]\cdot16H_2O$). FT-IR: 1004(m), 948(s), 906(s), 889(s), 826(s), 767(s), 727(s), 541(m), 525(m), 476(m) (cm^{-1}). Elemental analysis (%); calcd. (found): Na 2.6 (2.2), K 3.8 (4.1),W 65.2 (63.6).

$K_6Na_7[Nd(SiW_{11}O_{39})_2]\cdot20H_2O$ (Nd-9a): The above synthetic procedure was followed by using 0.1315 g (0.3 mmol) of $Nd(NO_3)_3\cdot6H_2O$ instead of $Pr(NO_3)_3\cdot6H_2O$. Yield: 0.1464 g, 57% (based on $Na_{10}[\alpha\text{-}SiW_9O_{34}]\cdot16H_2O$). FT-IR: 1006(m), 949(s), 906(s), 891(s), 826(s), 768(s), 729(s), 540(m), 526(m), 477(m) (cm^{-1}). Elemental analysis (%); calcd. (found): Na 2.6 (2.3), K 3.8 (4.3),W 65.2 (63.8).

$K_6Na_7[Sm(SiW_{11}O_{39})_2]\cdot24H_2O$ (Sm-10a): The above synthetic procedure was followed by using 0.1333 g (0.3 mmol) of $Sm(NO_3)_3\cdot6H_2O$ instead of $Pr(NO_3)_3\cdot6H_2O$. Yield: 0.1423 g, 56% (based on $Na_{10}[\alpha\text{-}SiW_9O_{34}]\cdot16H_2O$). FT-IR: 1008(m), 949(s), 909(s), 890(s), 830(s), 766(s), 725(s), 540(m), 521(m), 478(m) (cm^{-1}). Elemental analysis (%); calcd. (found): Na 2.6 (2.1), K 3.7 (4.1),W 64.4 (63.9).

Results and Discussion

Syntheses and structure

All the title compounds were synthesized following a single step reaction of $Na_{10}[\alpha\text{-}SiW_9O_{34}]\cdot16H_2O$ with $Ln(NO_3)_3\cdot nH_2O$ in potassium acetate buffer at pH 4.5. Syntheses process is very similar to our previously reported germanotungstates[13f] analogy. The trilacunary $[\alpha\text{-}SiW_9O_{34}]^{10-}$ anion easily undergoes transformation to monolacunary $[\alpha\text{-}SiW_{11}O_{39}]^{8-}$ anion at lower pH (4.5). The title anion is the assembly of two lanthanoid cations which are bridged by two acetate ligands in a $\mu_2:\eta^2-\eta^1$ mode, followed by the addition of two monolacunary $[\alpha\text{-}SiW_{11}O_{39}]^{8-}$ anion in a sandwich type manner acting as a tetra dentate ligand and two terminal water molecules coordinated with lanthanoid cations.

Single crystal X-ray diffraction studies of **Eu-1a** - **Tm-7a** reveals that the isolated compounds are isostructural. In the solid state two monolacunary $[\alpha\text{-}SiW_{11}O_{39}]^{8-}$ anions

are linked together by two lanthanoid cations; in addition each lanthanoid ion is coordinated to acetate chelator. The bridging of two acetate ligands to the lanthanoid cations in a $\mu_2{:}\eta^2–\eta^1$ modes are commonly seen, in polyoxometalates chemistry. Where each lanthanoid cation is eight coordinated, representing a square antiprismatic geometry (pseudo-D$4d$). The geometry of each lanthanoid ion is completed by its four coordination sites from monolacunary [α- SiW$_{11}$O$_{39}$]$^{8-}$ anion, three from two acetate ligands, and the remaining by a terminal water molecule [see **Fig. 1**].

Table 1 Crystallographic data information for **Eu-1a** to **Tm-7a**   POMs

	Eu-1	Gd-2	Tb-3	Dy-4	Ho-5	Er-6	Tm-7
Formula	$C_4H_6Eu_2K_8$ $Na_4O_{110}Si_2$ W_{22}	$C_4H_6Gd_2K_8$ Na_4 $O_{110}Si_2W_{22}$	$C_4H_6Tb_2K_8$ $Na_4O_{110}Si_2$ W_{22}	$C_4H_6Dy_2K_8$ $Na_4O_{110}Si_2$ W_{22}	$C_4H_6Ho_2K_8$ $Na_4O_{110}Si_2$ W_{22}	$C_4H_6Er_2K_8$ $Na_4O_{110}Si_2$ W_{22}	$C_4H_6Tm_2K_8$ $Na_4O_{110}Si_2$ W_{22}
FW	6623.65	6634.22	6637.57	6644.73	6649.59	6654.25	6657.59
Crystal system	monoclinic	monoclinic	monoclinic	monoclinic	monoclinic	monoclinic	monoclinic
Space group	P2$_1$/c	P2$_1$/c	P2$_1$/c	P2$_1$/c	P2$_1$/c	P2$_1$/c	P2$_1$/c
a/Å	20.1241(6)	20.0905(6)	20.1394(8)	20.1061(7)	20.0715(6)	20.0503(6)	20.0790(11)
b/Å	12.6661(3)	12.6729(3)	12.6367(4)	12.6303(3)	12.6297(4)	12.6340(2)	12.6152(4)
c/Å	21.1544(5)	21.0974(6)	21.1096(8)	21.1101(7)	21.0663(7)	21.0876(6)	21.0766(11)
β( )	110.377(3)	110.470(3)	110.718(4)	110.769(4)	110.526(4)	110.788(3)	110.904(7)
V/Å	5054.7(2)	5032.3(2)	5024.9(3)	5012.5(3)	5001.2(3)	4994.1(2)	4987.3(4)
Z	2	2	2	2	2	2	2
T/K	183(2)	183(2)	183(2)	183(2)	183(2)	183(2)	183(2)
D$_c$/Mg m^{-3}	4.352	2.189	4.387	4.403	2.208	4.421	4.433
μ/mm^{-1}	26.633	13.411	26.950	27.097	13.623	27.381	27.514
Goof(on F^2)	1.199	1.072	1.127	1.096	1.263	1.076	1.143
F(000)	5776	2890	5784	5788	2896	5796	5800
R$_1$[I >2σ(I)]^a	0.0560	0.0520	0.0409	0.0516	0.0532	0.0449	0.0684
wR$_2$ (all data)^b	0.1344	0.1277	0.0739	0.1155	0.1329	0.1071	0.1427

[a] $R = \sum||FoI - IFcII/\sum IFoI$. [b] $R_w = [\sum w(Fo^2 -Fc^2)^2/\sum w(Fo^2)^2]^{1/2}$

Such structural complexes were reported earlier by Milane et al for silicotungstate on dissolution of K$_5$[Ln-(SiW$_{11}$O$_{39}$)(H$_2$O)$_2$]· 24H$_2$O (Ln = Gd^{III} and Yb^{III}) in 2M potassium acetate buffer, where no crystal structure was reported for Gd^{III} - POMs and later one of us developed a single step synthetic protocol to isolate series of germanotungstate analogues. We followed the same synthetic protocol to study the reactivity of lanthanoids along the series with interaction of trilacunary silicotungstate polyanions in 1M potassium acetate buffers. Later, Wang et al reported on acetate chelated phosphotungstate dimer on interaction of trilacunary (PW$_9$O$_{34}$) ligands with lanthanoid

cations in sodium acetate buffer. Alkali cations were exchanged with organic ligands to isolate quality crystal for single crystal X-ray diffraction.

Same methodology was used at identical reaction condition for the earlier lanthanoid salts in the group. From FTIR analysis it was evident that no acetate ligand bridged to the isolated complexes. A single crystal X-ray diffraction studies of the compound **Nd-9a** and **Sm-10a** shows that the compounds are pure inorganic dimeric complex [Ln(α-SiW$_{11}$O$_{39}$)$_2$]$^{13-}$ [Ln = Nd^{III} (**Nd-9**), Sm^{III} (**Sm-10**)], where the geometry of the lanthanoids cation is in antiprismatic form. The two polyanion (SiW$_{11}$O$_{39}$) acts as a tetradentate ligand coordinated to four oxygen atom of each ligand [see **Fig. 2**]. Such type of complexes were earlier reported for Cerium K$_{4.5}$Na$_4$(H$_3$O)$_{3.5}$[Ce(SiW$_{11}$O$_{39}$)$_2$]·23H$_2$O,[27(a)]
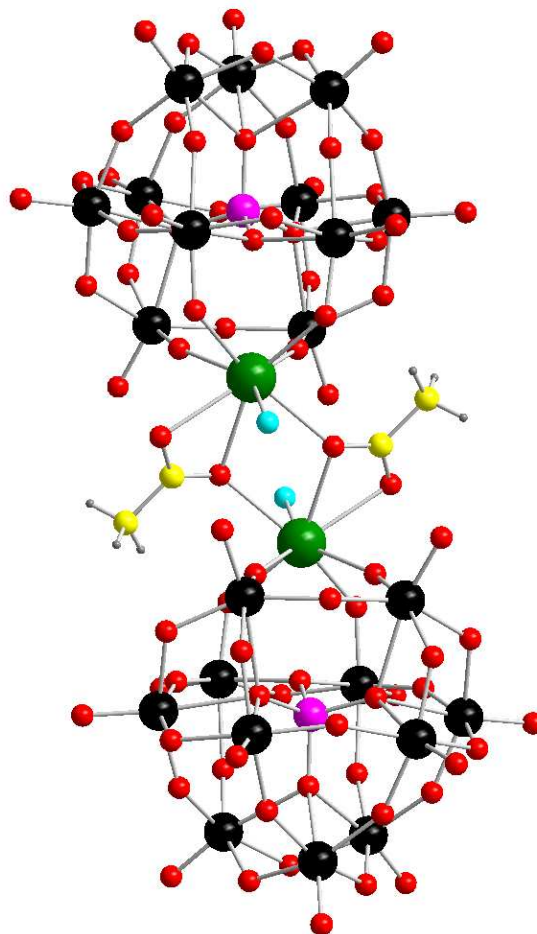
Fig.1 Ball and stick representation of the polyanion [{Ln(α-SiW$_{11}$O$_{39}$)(H$_2$O)}$_2$(μ-CH$_3$COO)$_2$]$^{12-}$ [Ln = Eu^{III} (**Eu-1**), Gd^{III} (**Gd-2**), Tb^{III} (**Tb-3**), Dy^{III} (**Dy-4**), Ho^{III} (**Ho-5**), Er^{III} (**Er-6**) and Tm^{III} (**Tm-7**)] (Color code: black: tungsten; red: oxygen; green:

lanthanoids; pink: silicon; yellow: carbon; grey: hydrogen, cations are omitted for clarity in figure).

Table 2: Single crystal X-ray crystallographic data for compound **Nd-9a** and **Sm-10a**.

Emp. Formula	$K_{5.5}Na_7O_{94}Si_2NdW_{22}$	$K_{5.5}Na_7O_{103}Si_2SmW_{22}$
Formula weight	6125.10	6275.21
Crystal system	Triclinic	Triclinic
Space group	P-1	P-1
a [Å]	12.7673(8)	12.7063(3)
b [Å]	16.6264(13)	16.5481(4)
c [Å]	23.2105(18)	23.1305(5)
α [ ]	94.958(7)	94.795(2)
β [ ]	99.502(6)	99.460(2)
γ [ ]	92.107(6)	92.393(2)
V [Å^3]	4834.7(6)	4772.98(19)
Z	2	2
ρ_{calcd} [g cm^{-3}]	4.208	4.366
μ [mm^{-1}]	26.979	27.411
Refelection collected	75960	75960
Unique (Rint) Obs.[$I > 2\sigma(I)$]	18281	23181
Parameters	671	707
Gof	1.037	1.071
R[$I > 2\sigma(I)$][a]	0.0734	0.0556
Rw(all data)[b]	0.2051	0.1354

[a] $R = \Sigma ||FoI - IFcII / \Sigma IFoI$. [b] $R_w = [\Sigma w(Fo^2 - Fc^2)^2 / \Sigma w(Fo^2)^2]^{1/2}$

$K_{6.5}H_{4.5}[CeK_2(SiW_{11}O_{39})_2]\cdot 26H_2O^{27b}$ and Pr-POM by Mialane et al on dissolution of $K_5[Pr-(SiW_{11}O_{39})]\cdot 26H_2O$ in 2M potassium acetate buffer, which were postulated previously by Blasse et al. for the europium complex $K_{13}[Eu(SiW_{11}O_{39})_2]$. Recently, Patzke et al synthesized and structurally characterized the 0D dimeric Eu-POM on interaction of $EuCl_3$ with trilacunary A-$[\alpha-SiW_9O_{34}]^{10-}$ in sodium acetate buffer, and also showed the role of Cs^+ cations at different concentration can lead to different structural motifs.[24]

Recently, our group reported on dimeric sandwich type $[Ln(PW_{11}O_{39})_2]^{11-}$ (Ln = Pr^{3+}, Nd^{3+}, Eu^{3+}, Gd^{3+}, Tb^{3+}, Dy^{3+}, Ho^{3+}, Er^{3+}, Tm^{3+}, and Yb^{3+}) complexes, which can be isolated either from dilacunary $[P_2W_{19}O_{69}(H_2O)]^{14-}$ or monolacunary $[\alpha-PW_{11}O_{39}]^{7-}$ on interaction with lanthanoid cations in 1M KOAc[13g]. Here, we followed a single pot rational synthesis to isolate these complexes from potassium acetate buffer. Nevertheless,

our current studies show that the coordination of earlier lanthanoids cation along the series behaves different to that of mid and late lanthanoid ions, which is attributed due to the decrease in atomic radius along the group due to lanthanoid contraction.
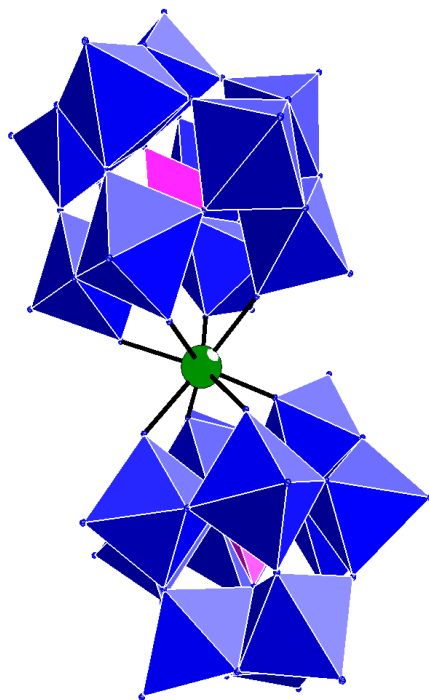
Fig.2 Ball and polyhedron representation of the polyanion $[Ln(\alpha\text{-}SiW_{11}O_{39})_2]^{13-}$ [Ln = Nd^{III} (**Nd-9**), Sm^{III} (**Sm-10**)], Color code: blue polyhedron: tungsten; green ball: lanthanoids; pink polyhedron: silicon.

FT-IR spectroscopy and thermogravimetric analysis

The FT-IR spectra of all isolated POMs **Eu-1a**, **Gd-2a**, **Tb-3a**, **Dy-4a**, **Ho-5a**, **Er-6a** and **Tm-7a** show similar characteristic asymmetric vibrations in the region of 1800 – 400 cm^{-1}, and their comparison clearly indicates that all the compounds are isostructural. The bands in the range of from 1000 to 400 cm^{-1} represent the "fingerprint region" of the POM ligands, and in this region there are four characteristic asymmetric vibrations which are attributed to $\nu_{as}(Si\text{-}O_a)$, terminal $\nu_{as}(W\text{-}O_t)$, corner-sharing $\nu_{as}(W\text{-}O_b\text{-}W)$, and edge-sharing $\nu_{as}(W\text{-}O_c\text{-}W)$. In the IR spectra the vibration bands at 1005 – 1008 cm^{-1} are assigned to $\nu_{as}(Si\text{-}O_a)$[28], and the bands at 952 – 954 cm^{-1} represent $\nu_{as}(W\text{=}O_t)$, and these bands are

considered as pure vibrations of POM ligands[29]. The frequencies in the range of 886 – 891 cm^{-1} corresponds to $v_{as}(W-O_b-W)$, and the bands at 811 – 814, 759 cm^{-1} can be attributed to $v_{as}(W-O_c-W)$. In addition, four characteristic vibrations in the range from 1624 cm^{-1} to 1398 cm^{-1}, are observed due to $v_{as}(C=O)$ and $v_{as}(C-O)$ groups of the acetate ligands which are bridged to the metal centres in a μ_2: $\eta^2 - \eta^1$ mode[13e,f, 25] [see **Fig. S1**]. On comparison of FT-IR spectra of isolated compounds with tri lacunary $Na_{10}[\alpha-SiW_9O_{34}]\cdot16H_2O$, and monolacunary $K_8[\alpha-SiW_{11}O_{39}]\cdot13H_2O$ ligand clearly indicates that at lower pH (4.5) the $[\alpha-SiW_9O_{34}]^{10-}$ anion easily transformed to the $[\alpha-SiW_{11}O_{39}]^{8-}$ anion, and this is in good accordance with previous literature[25,29] [see **Fig. S2**]. The FT-IR spectra of compounds (**Pr-8a**), Nd^{III} (**Nd-9a**), Sm^{III} (**Sm-10a**)] POM compounds shows similar asymmetric stretching vibrations in the region 1800 – 400 cm^{-1}. Bands attributed to $v_{as}(W-O_c-W)$ vibrations appeared at frequency 826, 767 and 724-728 cm^{-1}, the vibration bands at 1004 – 1008 cm^{-1} are assigned to $v_{as}(Si-O_a)$[28], and the bands at 948 – 954 cm^{-1} represent $v_{as}(W=O_t)$, these bands are considered to be the pure vibrations of the parent anion [see **Fig. S3**].

The thermogravimetric (TG) analyses of all these compounds were performed from room temperature to 700 $^{\circ}$C under nitrogen flowing atmosphere with the 5 $^{\circ}$C min^{-1} heating rate. The TG curves of **Eu-1a** – **Tm-7a** compounds show two steps of weight loss associated with loss of crystal water molecules and acetate ligands bridging between two NaK-{Ln-SiW₁₁} polyanions [see **Fig. S6**]. For the compounds **Eu-1a**, **Gd-2a**, **Tb-3a**, **Dy-4a**, **Ho-5a**, **Er-6a** and **Tm-7a**, the first step weight loss of 8.0, 5.81, 6.41, 8.60, 7.45, 7.59 and 7.52 % from room temperature to ~250 $^{\circ}$C corresponds to loss of 30, 24, 24, 32, 28, 28 and 28 water molecules respectively (two in coordination and remaining in crystal lattice). The second step weight loss of 1.87, 2.34, 0.87, 2.66, 1.82, 1.75 and 0.45 % up to ~600 $^{\circ}$C is attributed to the loss of two acetate ligands in all the compounds. In the TGA plots of complex (**Pr-8a**), Nd^{III} (**Nd-9a**), Sm^{III} (**Sm-10a**)] compounds only single step weight loss is found due to loss of crystalline water molecules. For **Pr-8a**, **Nd-9a** and **Sm-10a** POM compounds the weight loss of 5.74, 5.61, 6.67 % from room temperature to ~250 $^{\circ}$C, is due to loss of 20, 20 and 24 water molecules, respectively [see **Fig. S7**].

UV-visible spectroscopy

The UV/vis spectra of all compounds **Eu-1a**, **Gd-2a**, **Tb-3a**, **Dy-4a**, **Ho-5a**, **Er-6a**, and **Tm-7a** were recorded in aqueous solution in the range from 800 to 190 nm. The absorption spectra in the range from 300 to 190 nm, display two characteristic bands centred at 193 - 200 nm and another one centred at 251 - 254 nm. The former higher energy strong absorption bands are assigned to $p\pi$-$d\pi$ charge-transfer transitions of terminal $O_t{\rightarrow}W$ bonds whereas the lower energy absorption bands are ascribed to $p\pi$-$d\pi$ charge-transfer transitions of the $O_{b,(c)}{\rightarrow}W$ bonds[25,28].

In solid UV/vis spectrum of **Dy-4a** two stronger absorptions also appear at 758 and 810 nm in the near-IR region indicating the $^6H_{15/2}{\rightarrow}^6F_{3/2}$ and $^6H_{15/2}{\rightarrow}^6F_{5/2}$ transitions of Dy^{3+} (**Dy-4a**) ion [see **Fig. S4**]. For, **Ho-5a** spectrum seven absorption bands centred at 418, 452, 468, 475, 486, 539 and 645 nm are assigned to the $^5I_8{\rightarrow}^5G_5$, $^5I_8{\rightarrow}(^5F_1, {}^5G_6)$, $^5I_8{\rightarrow}^3K_8$, $^5I_8{\rightarrow}^5F_2$, $^5I_8{\rightarrow}^5F_3$, $^5I_8{\rightarrow}(^5F_4, {}^5S_2)$ and $^5I_8{\rightarrow}^5F_5$ transitions of the Ho^{3+}(**Ho-5a**) ion, but only the $^5I_8{\rightarrow}(^5F_1, {}^5G_6)$ and $^5I_8{\rightarrow}(^5F_4, {}^5S_2)$ transitions contribute to the color of this compound as mentioned in our previous literature [see **Fig. 3a**][28]. Similarly, for **Er-6a** spectrum seven absorption bands centred at 379, 408, 450, 488, 522, 544 and 654 nm are ascribed to $^4I_{15/2}{\rightarrow}^4F_{11/2, \ (5/2)}$, $^4I_{15/2}{\rightarrow}^2F_{9/2}$, $^4I_{15/2}{\rightarrow}^4F_{3/2}$, $^4I_{15/2}{\rightarrow}^4F_{7/2}$, $^4I_{15/2}{\rightarrow}(^4G_{11/2}, {}^4H_{11/2})$, $^4I_{15/2}{\rightarrow}^4S_{3/2}$ and $^4I_{15/2}{\rightarrow}^4F_{9/2}$ transitions of the Er^{3+}(**Er-6a**) ion, respectively [see **Fig. 3b**][30-32].
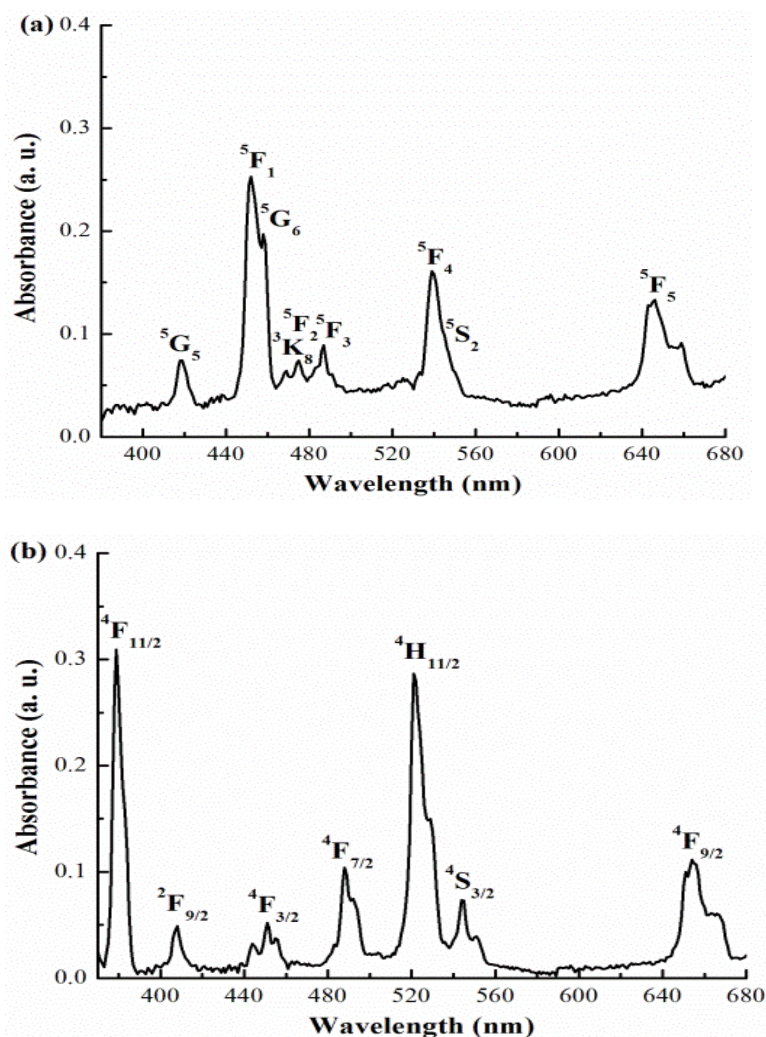
Fig. 3 Solid UV/vis spectra of **Ho-5** (3a) and **Er-6** (3b).

Photoluminescence spectroscopy

The photoluminescence spectra of compounds **Eu-1a**, **Gd-2a**, **Tb-3a**, **Dy-4a**, **Ho-5a**, **Er-6a**, and **Tm-7a** were investigated on photoexcitation at room temperature. The emission spectrum of **Eu-1** display red photoluminescence on photoexcitation at 394 nm, with five characteristic emission peaks centred at 584, 596, 618, 654 and 704 nm, which are assigned to the $^5D_0{\rightarrow}^7F_0$, $^5D_0{\rightarrow}^7F_1$, $^5D_0{\rightarrow}^7F_2$, $^5D_0{\rightarrow}^7F_3$ and $^5D_0{\rightarrow}^7F_4$ transitions of Eu^{3+} ion, respectively [see **Fig. 4a**][25]. Generally, the transition $^5D_0{\rightarrow}^7F_0$ is symmetric forbidden but the peak observed at 584 nm indicates that the Eu^{3+} ions in **Eu-1a** POM

occupies with low symmetry and have no inversion centre. The emission transitions $^5D_0\rightarrow^7F_{(1,3)}$ are magnetic-dipolar transitions, so intensity of these transitions varies with the field strength of ligands acting on the Eu^{3+} ion. Likewise, the transitions $^5D_0\rightarrow^7F_{(0,2,4)}$ are electric-dipolar transitions, which are very sensitive to the chemical bonds in the close proximity of the Eu^{3+} ion[28]. The emission spectrum of **Tb-3a**, shows green photoluminescence under excitation at 330 nm, with the three characteristic emission bands which are assigned to $^5D_4\rightarrow^7F_5$ (546 nm) $^5D_4\rightarrow^7F_4$ (584) and $^5D_4\rightarrow^7F_3$ (623 nm) transitions of the Tb^{3+} ion [see **Fig. S5**]. The emission transition $^5D_4\rightarrow^7F_5$ is an electric-dipolar transition so this is very sensitive to change in the chemical bonds in the vicinity of Tb^{3+} ion. The intense emission transition $^5D_4\rightarrow^7F_5$ at 546 nm is just because off decrease in the site symmetry of Tb^{3+} ion in complex, as previously reported in our work[28]. Similarly, the emission spectrum of **Dy-4a** displays three emission peaks at 482, 575 and 664 nm, under the photo excitation at 370 nm. The emission transitions are assigned to the $^4F_{9/2}\rightarrow^6H_{15/2}$ (blue emission), $^4F_{9/2}\rightarrow^6H_{13/2}$ (yellow emission) and $^4F_{9/2}\rightarrow^6H_{11/2}$ transitions of Dy^{3+} ion [see **Fig. 4b**]. From emission spectrum the intensity of yellow emission transition $^4F_{9/2}\rightarrow^6H_{13/2}$ at 575 nm, is stronger than the blue emission transition $^4F_{9/2}\rightarrow^6H_{15/2}$ at 482 nm suggesting that the $[\alpha\text{-}SiW_{11}O_{39}]^{8-}$ ligand is suitable for the sensitization of yellow luminescence for Dy^{3+} ion[33-35], photoexcitation at 377 nm for **Sm-10a** shows three emission peaks centered at 563, 597 and 647 nm. These emissions are due to $^4G_{5/2}\rightarrow^6H_{5/2}$, $^4G_{5/2}\rightarrow^6H_{7/2}$ and $^4G_{5/2}\rightarrow^6H_{9/2}$ transitions of Sm^{3+} ion. The emission $^4G_{5/2}\rightarrow^6H_{7/2}$ at 597 nm is most intense peak these observations are in good accordance with the previous reports[36] [see **Fig. 5**].
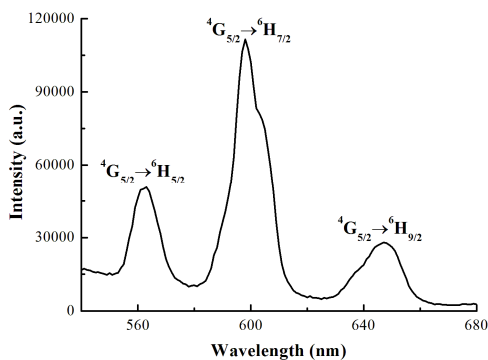
Fig. 4 Photoluminescence spectra of **Eu-1a** (4a) and **Dy-4a** (4b) in room temperature on excitation at 394 and 370 nm wavelengths.
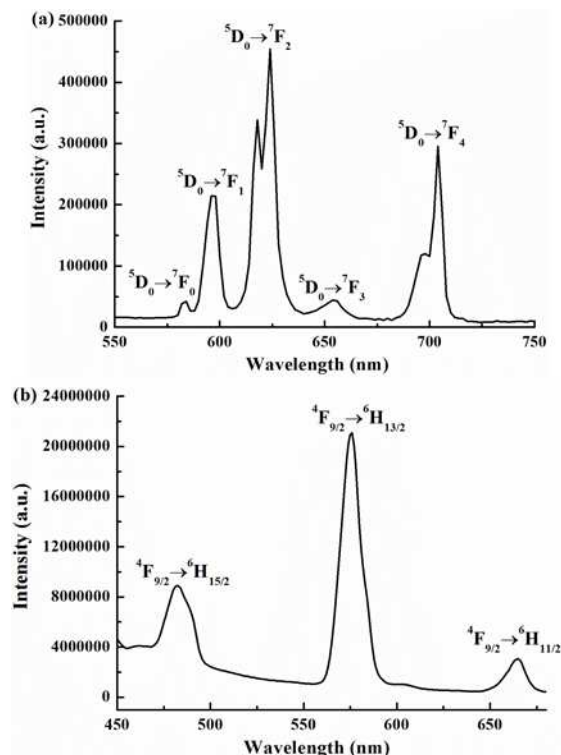
Fig. 5 Photoluminescence spectra of **Sm-10** at room temperature on excitation at 377 nm wavelength.

NMR Spectroscopy

The ^{13}C NMR spectra for compound **Eu-1a** and ^{1}H NMR spectra for compounds **Eu-1a, Gd-2a**, **Tb-3a**, **Dy-4a**, **Ho-5a**, **Er-6a** and **Tm-7a** were recorded at a 400 MHz magnetic field at 298 K. All the samples were prepared by redissolving the isolated crystals in D_2O. A ^{13}C NMR spectrum of the molecular complexes **Eu-1a** shows two signals, at δ 22.72 and 182.39 ppm respectively. The downfield ^{13}C signals are due to the oxygen-bound carbon atoms (See Fig S9). The ^{1}H NMR spectra of the molecular complexes **Eu-1a, Gd-2a, Tb-3a, Dy-4a, Ho-5a, Er-6a and Tm-7a** show one singlet at δ 1.79, 1.81, 1.86, 2.19, 1.88, 1.96, and 1.96 ppm respectively, corresponding to the protons of methyl groups (See Fig S10).[37]

Magnetic properties

The magnetic properties of compounds **Gd-2a**, **Tb-3a**, **Dy-4a**, **Ho-5a**, **Er-6a** and **Tm-7a** were studied at room temperature, the analysis of magnetization plots using Microsense

ADE-EV9 vibrating sample magnetometer (VSM). All these compounds exhibits paramagnetic behaviour with saturation magnetization about 0.107, 0.233, 0.264, 0.245, 0.213 and 0.129 emu/g for **Gd-2a**, **Tb-3a**, **Dy-4a**, **Ho-5a**, **Er-6a** aand **Tm-7** respectively [see **Fig. 6**].
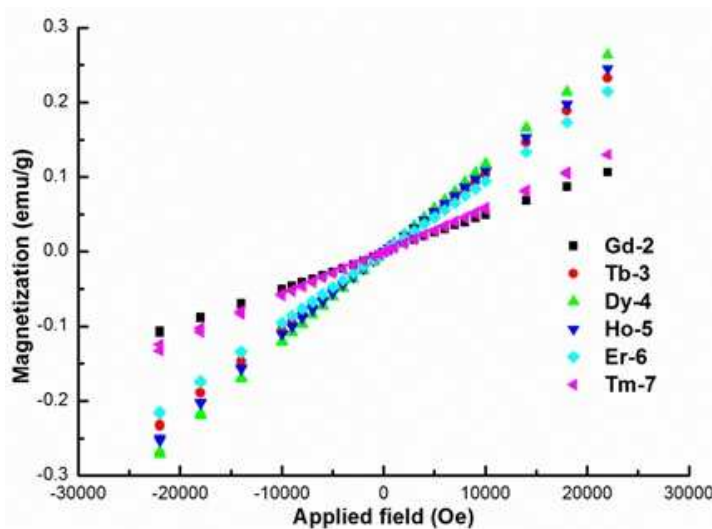
Fig. 6 Magnetization curves of **Gd-2a**, **Tb-3a**, **Dy-4a**, **Ho-5a**, **Er-6a** and **Tm-7a.**

Conclusions

In conclusion we have isolated a series of dimeric complexes of lanthanoid-containing Keggin-type silicotungstates: $[\{Ln(\alpha\text{-}SiW_{11}O_{39})(H_2O)\}_2(\mu\text{-}CH_3COO)_2]^{12-}$ [Ln = Eu^{III} (**Eu-1**), Gd^{III} (**Gd-2**), Tb^{III} (**Tb-3**), Dy^{III} (**Dy-4**), Ho^{III} (**Ho-5**), Er^{III} (**Er-6**) and Tm^{III} (**Tm-7**)] and $[Ln(\alpha\text{-}SiW_{11}O_{39})_2]^{13-}$ [Ln = Pr^{III} (**Pr-8**), Nd^{III} (**Nd-9**), Sm^{III} (**Sm-10**)],following a single step reaction of $Na_{10}[\alpha\text{-}SiW_9O_{34}]\cdot16H_2O$ with $Ln(NO_3)_3\cdot nH_2O$ in potassium acetate buffer at pH 4.5. All these compounds were structurally characterized by single-crystal X-ray diffraction and other analytical techniques including FT-IR, ICP-AES,

UV/vis, photoluminescence spectroscopy, thermogravimetric analysis and VSM. Our studies show that the coordination of earlier lanthanoids cation along the series behaves different to that of mid and late lanthanoid ions, due to lanthanoid contraction. **Eu-1**, **Tb-3**, **Dy-4** and **Sm-10** compounds show good photoluminescence properties at room temperature. VSM studies at room temperature exhibits paramagnetic behaviour for **Gd-2**, **Tb-3**, **Dy-4**, **Ho-5**, **Er-6** and **Tm-7**, in the presence of applied magnetic field.

Acknowledgements

Notes and references

[a] Department of Chemistry, University of Delhi, North Campus, Delhi, India, Fax: +91 11 2766 6605; Tel: +91 11 27666646; E-mail: fhussain@chemistry.du.ac.in
[b]INMAS, Lucknow Road, Delhi, India.

†Electronic Supplementary Information (ESI) available: [details of any supplementary information available should be included here]. See DOI: 10.1039/b000000x/

‡ A single crystal suitable for X-ray diffraction for compounds Eu^{III} (**Eu-1**), Gd^{III} (**Gd-2**), Tb^{III} (**Tb-3**), Dy^{III} (**Dy-4**), Ho^{III} (**Ho-5**), Er^{III} (**Er-6**) Tm^{III} (**Tm-7**), and (**Pr-8**), Nd^{III} (**Nd-9**), Sm^{III} (**Sm-10**) were mounted on a capillary tube for indexing and intensity data collection at 183(2) K on an Oxford Xcalibur CCD single-crystal diffractometer (MoKα radiation, λ = 0.71073 Å)[38] (see Table 1 and 2). Pre-experiment, data collection, data reduction and analytical absorption corrections[39] were performed with the Oxford

program suite *CrysAlisPro*.[40] The crystal structures were solved with SHELXS-97[41] using direct methods. The structure refinements were performed by full-matrix least-squares on F^2 with SHELXL-97.[41] All programs used during the crystal structure determination process are included in the WINGX software.[42] Crystallographic data for the structure compounds **Eu-1**, **Gd-2**, **Tb-3**, **Dy-4**, **Ho-5**, **Er-6** and **Tm-7** have been deposited with the Cambridge Crystallographic Data Center (CCDC) under the number 983094-983100. Copies of the data can be obtained, free of charge, on application to CCDC 12 Union Road, Cambridge CB2 1EZ, UK [Fax: +44-1223-336033; e-mail: deposit@ccdc.cam.ac.uk or at www.ccdc.cam.ac.uk]. Crystallographic data for the structure compounds **Nd-9** and **Sm-10** have been deposited with FIZ-Karlsruhe, Further details on the crystal structure data may be obtained from the Fachinformationszentrum Karlsruhe, 76344 Eggenstein-Leopoldshafen, Germany (fax: (+49) 7247-808-666; e-mail: crysdata@fiz-karlsruhe.de), on quoting the depository number CSD-427456 and CSD-427457. Largest diff.peak and hole 13.83 eA°⁻³ - 1.02A° from O20 and -4.26 eA°⁻³ – 0.47 A° from W2 for (**Nd-9**) and 9.02 eA°⁻³ - 0.84A° from O10 and -4.66 eA°⁻³ – 0.67 A° from W2 for. Disorder of cations and crystal waters are common phenomenon in polyoxometalate chemistry.

1 M. T. Pope, Heteropoly and Isopoly Oxometalates, *Springer-Verlag*, Berlin, 1983.

2 C. L. Hill and C. M. Prosser-McCartha, *Coord. Chem. Rev.*, 1995, **43**, 407.

3 D. E. Katsoulis, *Chem. Soc. Rev.*, 1998, **98**, 359.

4 B. Keita and L. Nadjo, *J. Mol. Catal. A: Chem.*, 2007, **262**, 190.

5 Y. Zhou, R. L. Bao, B. Yue, M. Gu, S. P. Pei and H. Y. He, *J. Mol. Catal. A: Chem.*, 2007, **270**, 50.

6 B. Hasenknopf, *Frontiers in Bioscience*, 2005, **10**, 275**.**

7 M. A. AlDamen, S. Cardona-Serra, J. M. Clemente-Juan, E. Coronado, A. Gaita-Ariño, C. Martí-Gastaldo, F. Luis and O. Montero, *Inorg. Chem.*, 2009, **48**, 3467.

8 Z. F. Li, W. S. Li, X. J. Li, F. K. Pei, Y. X. Li and H. Lei, *Magn. Reson. Imaging*, 2007, **25**, 412.

9 T. Yamase, M. T. Pope, Polyoxometalate Chemistry for Nano-composite Design, *Kluwer*, Dordrecht, 2002.

10 D. L. Long, E. Burkholder and L. Cronin, *Chem. Soc. Rev.*, 2007, **36**, 105.

11 K. Wassermann, M. H. Dickman and M. T. Pope, *Angew. Chem. Int. Ed.*, 1997, **36**, 1445.

12 B. S. Bassil, M. H. Dickman, I. Romer, B. von der Kammer and U. Kortz, *Angew. Chem. Int. Ed.*, 2007, **46**, 6192.

13 (a)F. Hussain, B. Spingler, F. Conrad, M. Speldrich, P. Kogerler, C. Boskovic and G. R. Patzke, *Dalton Trans.*, 2009, 4423; (b) F. Hussain, R. W. Gable, M. Speldrich, P. Kogerler and C. Boskovic, *Chem. Commun.*, 2009, 328; (c) F. Hussain, F. Conrad and G. R. Patzke, *Angew. Chem. Int. Ed.*, 2009, **48**, 9088; (d) F. Hussain and G. R. Patzke, *CrystEngComm*, 2011, **13**, 530; (e) F. Hussain, A. Degonda, S. Sandriesser, T. Fox, S. S. Mal, U. Kortz and G. R. Patzke, *Inorg. Chim. Acta*, 2010, **363**, 4324; (f) F. Hussain, S. Sandriesser, M. Speldrich and G. R. Patzke, *J. Solid State Chem.*, 2011, **184**, 214; (g) R. Gupta, M. K. Saini, F. Doungmene, P. de Oliviera, F. Hussain, *Dalton Trans*., 2014, **43 (22),** 8290 – 8299.

14 R. D. Peacock and T. J. R. Weakley, *J. Am. Chem. Soc. A*, 1971, 1836.

15 M. Sadakane, M. H. Dickman and M. T. Pope, *Angew. Chem. Int. Ed.*, 2000, **39**, 2914.

16 P. Mialane, L. Lisnard, A. Mallard, J. Marrot, E. Antic-Fidancev, P. Aschehoug, D. Vivien and F. Secheresse, *Inorg. Chem.*, 2003, **42**, 2102.

17 P. Mialane, A. Dolbecq, E. Riviere, J. Marrot and F. Secheresse, *Eur. J. Inorg. Chem.*, 2004, 33.

18 J. Y. Niu, J. W. Zhao and J. P. Wang, *Inorg. Chem. Commun.*, 2004, **7**, 876.

19 J. P. Wang, J. W. Zhao, X. Y. Duan and J. Y. Niu, *Cryst. Growth Des.*, 2006, **6**, 507.

20 F. Y. Li, L. Xu, Y. G. Wei, G. G. Gao, L. H. Fan and Z. K. Li, *Inorg. Chim. Acta*, 2006, **359**, 3795.

21 B. S. Bassil, M. H. Dickman, B. von der Kammer and U. Kortz, *Inorg. Chem.*, 2007, **46**, 2452.

22 D. Y. Du, J. S. Qin, S. L. Li, Y. Q. Lan, X. L. Wang and Z. M. Su, *Aust. J. Chem.*, 2010, **63**, 1389.

23 H. Y. An, H. Zhang, Z. F. Chen, Y. G. Li, X. Liu and H. Chen, *Dalton Trans.*, 2012, **41**, 8390.

24 L. B. Ni, B. Spingler, S. Weyeneth and G. R. Patzke, *Eur. J. Inorg. Chem.*, 2013, 1681.

25 J. Niu, K. Wang, H. Chen, J. Zhao, P. Ma, J. Wang, M. Li, Y. Bai and D. Dang, *Cryst. Growth Des.*, 2009, **9**, 4362.

26 A. Tézé, G. Hervé, R. G. Finke, D. K. Lyon, *Inorg. Synth.*, 1990, **27**, 85.

27 (a) R. Q. Sun, H. H. Zhang, S. L. Zhao, C. C. Huang and X. L. Zheng, *Chin. J. Struct. Chem.*, 2001, **20**, 413; (b) J. Y. Niu, Z. L. Wang and J. P. Wang, *J. Coord. Chem.*, 2003, **56**, 895.

28 L. B. Ni, F. Hussain, B. Spingler, S. Weyeneth and G. R. Patzke, *Inorg. Chem.*, 2011, **50**, 4944.

29 C. R. Deltcheff, M. Fournier, R. Frank and R. Thouvenot, *Inorg. Chem.*, 1983, **22**, 207.

30 H. Naruke, J. Iijima and T. Sanji, *Inorg. Chem.*, 2011, **50**, 7535.

31 C. M. Granadeiro, R. A. S. Ferreira, P. C. R. Soares-Santos, L. D. Carlos and H. I. S. Nogueira, *Eur. J. Inorg. Chem.*, 2009, 5088.

32 J. Y. Niu, J. W. Zhao and J. P. Wang, *J. Mol. Struct.*, 2004, **701**, 19.

33 S. W. Zhang, Y. Wang, J. W. Zhao, P. T. Ma, J. P. Wang and J. Y. Niu, *Dalton Trans.*, 2012, **41**, 3764.

34 S. W. Zhang, J. W. Zhao, P. T. Ma, H. N. Chen, J. Y. Niu and J. P. Wang, *Cryst. Growth Des.*, 2012, **12**, 1263.

35 Y. Q. Sun, J. Zhang, Y. M. Chen and G. Y. Yang, *Angew. Chem. Int. Ed.*, 2005, **44**, 5814.

36 S. Zhang, J. Zhao, P. Ma, H. Chen, J. Niu and J. Wang, *Cryst. Growth Des.*, 2012, **12**, 1263.

37 F. Hussain, A. Degonda, S. Sandriesser, T. Fox, S. S. Mal, U. Kortz and G. R. Patzke, *Inorg. Chim. Acta*, 2010, **363**, 4324-4328.

38 Xcalibur CCD System; Oxford Diffraction Ltd: Abingdon, Oxfordshire, England, 2007.

39 R. C. Clark and J. S. Reid *Acta Cryst.* 1995, **A51**, 887-897.

40 *CrysAlisPro* (versions 1.171.34.49), Oxford Diffraction Ltd, Abingdon, Oxfordshire, England.

41 G. M. Sheldrick *Acta Cryst.* 2008, **A64**, 112-122.

42 L. J. Farrugia *J. Appl. Cryst.* 2012*, **45**, 849-854.